Med Biol Eng Comput (2010) 48:589–595
DOI 10.1007/s11517-010-0612-3

ORIGINAL ARTICLE

Fully automatic initialization method for quantitative assessment of chest-wall deformity in funnel chest patients

Ho Chul Kim · Hyung Joo Park · Kyoung Won Nam · Soo Min Kim · Eun Jeong Choi · Seungoh Jin · Jae-Jo Lee · Sang Woo Park · Hyuk Choi · Min Gi Kim

Received: 25 November 2009 / Accepted: 7 April 2010 / Published online: 21 April 2010

Abstract In our previous study, we developed a computerized technique that measured degree of chest-wall deformity in funnel chest patients using several image processing techniques, such as, active contour model. It could calculate quantitative indices for chest-wall deformity using patient's CT image. However, the algorithm contained manual initialization processes that required clinicians to obtain additional training processes to understand engineering contents and be familiar with the technique. In this study, we suggested a fully automatic algorithm that can measure the degree of chest-wall deformity by automating initialization processes. The initialization processes to segment CT images were automated by applying various image processing techniques such as histogram analysis, point detection, and object recognition. In order to evaluate the performance of the proposed algorithm, both the previous algorithm (semi-automatic) and newly suggested algorithm (fully automatic) were applied to preoperative CT images of 61 funnel chest patients to calculate several indices that represented chest-wall deformity quantitatively and to measure their processing time of our algorithm using a computer. The time required for initialization processes was 28.12 s using the semi-automatic algorithm and 0.07 s using the fully automatic algorithm (99.75% speed enhancement) and the time required for whole index calculation process was 61.12 s in semi-automatic algorithm and 30.09 s in fully automatic algorithm (50.76% speed enhancement). In most indices, calculation results of the two algorithms showed no significant difference between each other. The proposed algorithm could calculate chest-wall deformity more accurately with relatively shorter processing time than our previous method. Applying this algorithm is expected to facilitate more efficient diagnosis and evaluation processes of funnel chest patients for clinical doctors.

Keywords Fully automatic initialization · Segmentation · Active contour model · Quantitative assessment index · Funnel chest · Chest-wall deformity

H. C. Kim · S. Jin · J.-J. Lee
Korea Electrotechnology Research Institute, Ansan, Korea
e-mail: tiger1005@gmail.com

H. J. Park
Department of Thoracic and Cardiovascular Surgery, College of Medicine, Korea University, Seoul, Korea

K. W. Nam
Biomedical Engineering Branch, National Cancer Center, Goyang, Korea

S. M. Kim · M. G. Kim (✉)
Department of Electronics and Information Engineering, Korea University (Sejong Campus), Jochiwon-eup, Yeongi-gun, Chungcheongnam-do, Jochiwon, Republic of Korea
e-mail: mgkim@korea.ac.kr

E. J. Choi
Department of Radiology, College of Medicine, Korea University, Seoul, Korea

S. W. Park
Department of Radiology, Konkuk University Hospital, Seoul, Korea

H. Choi
Department of Biomedical Engineering, Brain Korea 21 Project for Biomedical Science, College of Medicine, Korea University, Seoul, Korea

1 Introduction

In order to establish a proper preoperative plan and evaluate postoperative results for funnel chest (pectus excavatum) surgery, quantitative measurement of chest-wall deformity of the funnel chest patient is important [1–4, 12, 13]. For this purpose, various indices such as Haller index (HI), vertebral index (VI), Frontosagittal Index (FSI), and depression index (DI) have been used clinically. [5, 6, 9, 12, 13] Traditionally, these indices are calculated manually by measuring required factors with a ruler from the patient's chest CT image, however, errors in calculation can be occur due to inaccurate manual measurement of required factors.

In order to solve this problem, our group suggested a computerized algorithm that extracts the degree of chest-wall deformity from a CT image using image processing techniques such as image segmentation and curve fitting, and also recommended four new indices that can be calculated using the suggested algorithm—eccentricity index (EI), flatness index (FI), circularity index (CI), and rotation index (RI) [8]. The proposed method demonstrated enhanced precision and processing time compared with manual calculation, yet it was not a fully automatic system; that is, to extract chest-wall boundary information from the CT image, initial values for image segmentation needed to be manually marked by an operator. This manual marking process was time-consuming and moreover, additional training and exercising procedures were necessary for clinicians to understand technical aspects of the algorithm to mark initial points appropriately.

In this study, we suggested an enhanced algorithm that automated overall initialization processes to calculate targeted index automatically. In order to automate initialization processes, several image processing techniques including histogram analysis and threshold method were adopted. In order to compare the performance of the newly suggested method (fully automatic) with the previous method (semi-automatic), both methods were applied to analyze preoperative CT images of 61 funnel chest patients to calculate HI, EI, FI, CI, and RI values and to measure the time required to complete the process.

2 Materials and Methods

2.1 Overview of the semi-automatic process

In the semi-automatic method, an operator must mark tens of initial points around the interested area (chest-wall) manually to extract boundary information from the Active Contour Model (ACM) [16, 17]. Next, the algorithm automatically connects these points by interpolation to construct an initial boundary curve (Blue line in Fig. 1a). After initialization, the algorithm performs ACM deformation process (Green lines in Fig. 1a) to extract inner boundary values of the chest-wall (Red lines in Fig. 1a). Based on these boundary values, indices that represent chest-wall deformity (EI, FI, CI, and RI) were calculated (Fig. 1b) automatically.

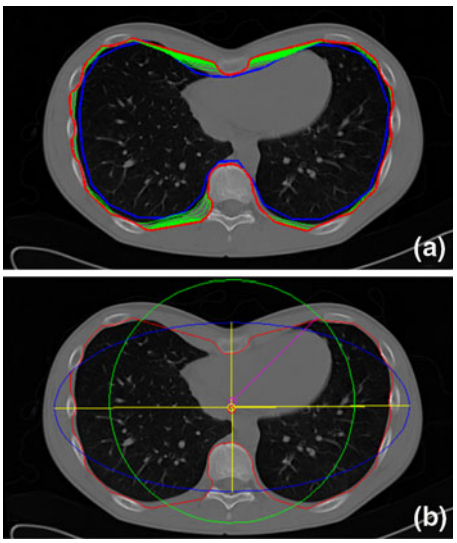

Fig. 1 Extraction of inner boundary values of the chest-wall (**a**) and calculation of indices that represent chest-wall deformity (**b**) using the semi-automatic method

2.2 Proposed auto-initialization process

First, the proposed auto-initialization algorithm rotated CT image to resister left and right chest-wall horizontally to calculate RI value accurately. To do this, it needed to be determined whether the chest-wall was inclined or not in the original CT image. In order to separate lung and rib areas, the proposed algorithm carried out histogram analysis of the image since the lung and rib have different histogram distribution. Setting proper threshold values, lung area (Fig. 2a), and rib area (Fig. 2b) were obtained from the original image. Then, from this extracted boundary information of left and right lungs, two boundary points which were located on vertically bottom position in left and right lungs were selected automatically to determine the inclined direction and angle of the chest-wall (Fig. 2c). Using this inclination information, the algorithm rotated the original CT image to arrange left and right lungs horizontally (Fig. 2d). After rotation, additional registration processes were performed to extract boundary information of lung, rib, sternum, and vertebra from the rotated CT image. At this time, interested areas were extracted from the CT image automatically by setting proper Hounsfield unit (HU) values to each image. Most CT images used in this study could be

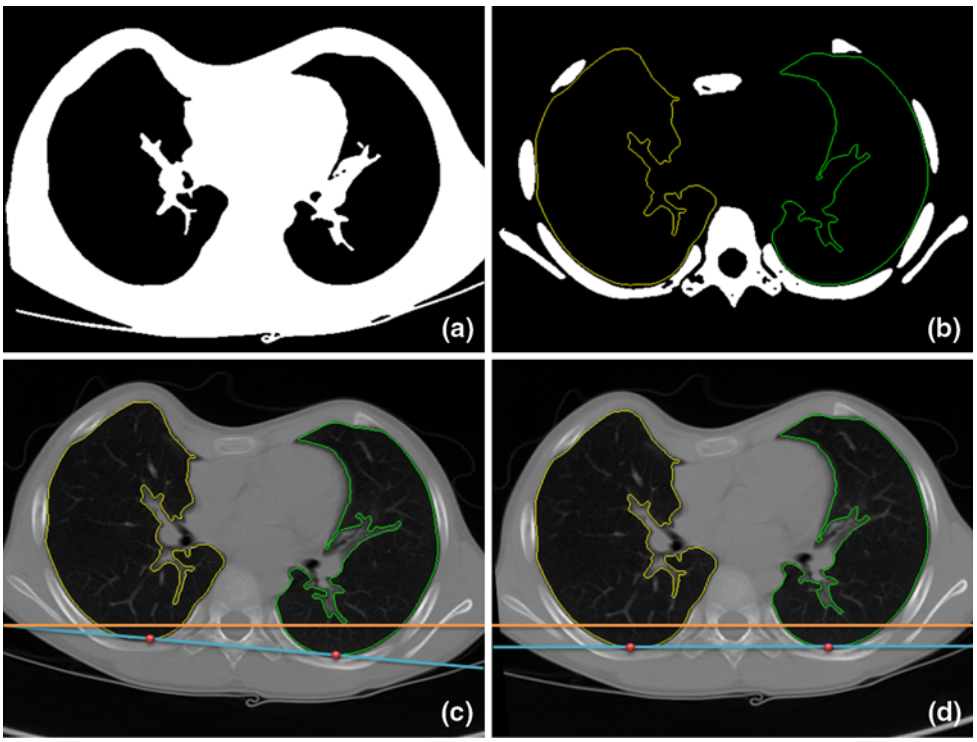

Fig. 2 Rotation of original CT image to arrange left and right lungs horizontally. **a** Extraction of lung area by histogram analysis. **b** Extraction of rib area by histogram analysis. **c** Calculation of inclined direction and angle. **d** Image after rotation

separated into lung and bone using standardized HU value, however, some CT images included noise signals generated by various environmental conditions, such as, the patient's movement during CT photographing and, therefore, additional HU value adjustment was needed. Preset range of HU values were 340–605 for lung and 1101–1156 for bone, respectively.

After pre-processing of the original CT image, the proposed algorithm produced an edge map and a gradient vector flow (GVF) field automatically and selected a point which was located on the vertically bottom position from boundary information of the sternum (Upper point in Fig. 3a). It also selected two boundary points from the left and right lung boundaries which were located in the closest position from the selected bottom point of the sternum, and connected three selected points through interpolation to form an upper boundary of initial boundary curve. Similarly, the proposed algorithm selected a top point of the vertebra (Lower point in Fig. 3a) and also selected two boundary points from left and right lung boundaries which were located on the closest from the selected top point of the vertebra. Then, it connected three selected points through interpolation to form the lower boundary of initial boundary curve. Integrating these upper and lower boundary lines and lung boundary information (Left and right curves in Fig. 3a), initial boundary curve for ACM deformation was created automatically (Fig. 3b). After setting initial boundary curve, the proposed algorithm performed ACM deformation process to extract boundary information of the inner chest-wall (Fig. 3c) and finally, calculated target indices (EI, FI, CI, and RI) through an additional curve fitting method (Fig. 3d).

2.3 Experimental setting for performance verification

In order to evaluate the performance of the newly suggested algorithm, we applied two algorithms (semi-automatic and fully automatic) to the preoperative CT images of 61 funnel chest patients. In semi-automatic measurements, an expert radiologist performed initialization processes manually. In order to compare experimental results of two algorithms, we calculated statistical correlation between two algorithms for each index. The hardware specification used was a Windows XP® installed PC with 3.00 GHz CPU and 2 GB RAM. Operating software used in this series of analysis was MATLAB 7.5®.

3 Experimental results

Table 1 shows the results of EI, FI, CI, and RI calculation using semi-automatic and fully automatic methods (among 61 patients, data of only 15 patients were listed). In fully automatic method, mean ± standard deviation were 0.87 ± 0.04 for EI, 0.52 ± 0.07 for FI, 0.35 ± 0.02 for CI,

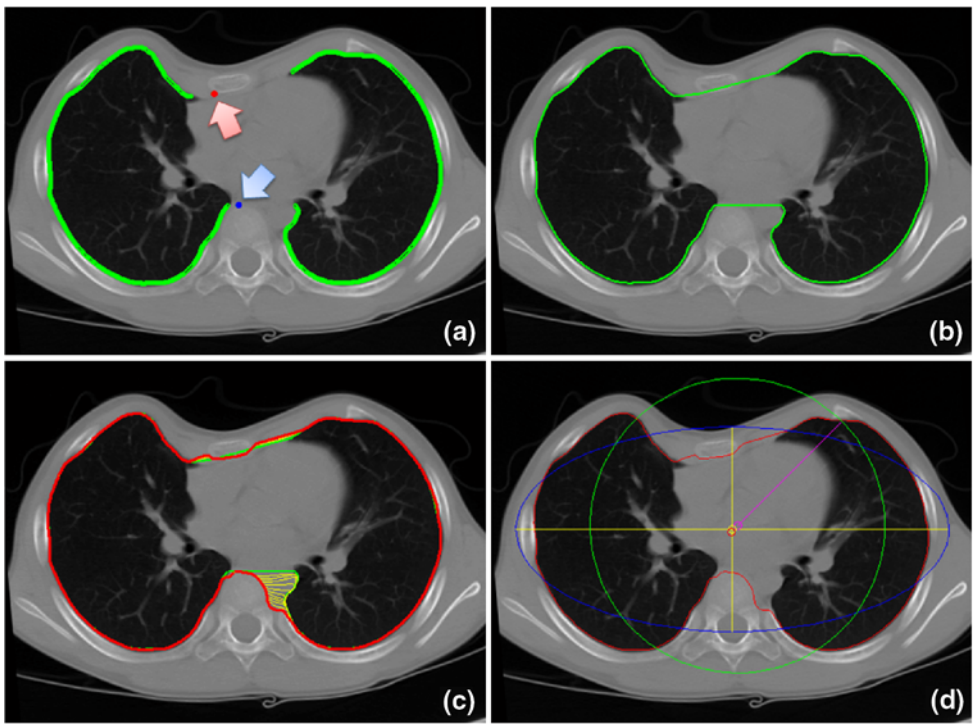

Fig. 3 Index calculation using the proposed auto-initialization method. **a** Selection of a bottom point of the sternum (*Upper point*) and a top point of the vertebra (*Lower point*). **b** Creation of initial boundary curve. **c** ACM deformation to extract Inner boundary of the chest-wall. **d** Index calculation processes (EI, FI, CI, and RI)

Table 1 Results of index calculation using fully automatic and semi-automatic methods in CT images of 15 funnel chest patients

ID	Gender	Age (year)	Fully automatic method				Semi-automatic method			
			EI	FI	CI	RI	EI	FI	CI	RI
1	M	7	0.88	0.53	0.34	−0.79	0.87	0.51	0.35	−1.26
2	F	9	0.89	0.54	0.34	3.22	0.87	0.51	0.35	1.83
3	M	6	0.88	0.53	0.34	0.29	0.88	0.53	0.35	0.37
4	M	4	0.89	0.54	0.34	0.17	0.87	0.51	0.35	2.20
5	M	21	0.87	0.51	0.35	3.56	0.87	0.50	0.36	2.62
6	M	5	0.87	0.51	0.35	4.27	0.87	0.51	0.35	3.52
7	M	5	0.87	0.51	0.35	−0.38	0.86	0.49	0.36	−0.04
8	M	19	0.92	0.61	0.31	1.75	0.90	0.57	0.34	1.52
9	M	5	0.89	0.54	0.34	0.75	0.88	0.52	0.35	1.55
10	M	12	0.89	0.54	0.34	−0.99	0.88	0.53	0.35	−1.37
11	M	11	0.90	0.57	0.34	1.49	0.89	0.54	0.35	1.93
12	F	8	0.88	0.52	0.35	2.47	0.87	0.50	0.36	3.11
13	M	4	0.89	0.54	0.34	−0.50	0.89	0.54	0.33	−1.93
14	M	4	0.89	0.55	0.33	−0.03	0.89	0.53	0.34	−0.73
15	F	24	0.89	0.54	0.33	4.89	0.88	0.52	0.35	5.39

and 1.10 ± 2.00 for RI. In semi-automatic method, mean $\pm$ standard deviation were 0.86 ± 0.04 for EI, 0.50 ± 0.07 for FI, 0.36 ± 0.02 for CI, and 0.86 ± 1.62 for RI. These results showed that mean EI, FI, and CI values were very similar to each other for both the methods; however, as a result of image rotation during use of the fully automatic method only, the difference in mean RI values between the two methods was relatively high. However, data from the Student *t*-test showed *P* values of 0.157 for EI, 0.125 for FI, 0.014 for CI, and 0.475 for RI, respectively, which meant that none of the index values showed a statistically significant difference at 0.01 threshold level between the two methods. Results of RI calculation showed a relatively high difference in mean

value; however, a relatively higher sample deviation in the Student *t*-test canceled out this statistical difference.

Pearson correlation coefficients between fully and semi-automatic algorithms were 0.9809 for EI, 0.9835 for FI, 0.9574 for CI, and 0.8474 for RI and *P* values were 1.1814E-43, 1.6019E-45, 1.5608E-33, and 7.3133E-18, respectively. As the Table 1 shows, correlation was relatively low in RI results. It is because that there is no image rotation process during initialization in the previous method, therefore, RI calculation of the previous method was inaccurate for the originally inclined CT images. However, original CT image was pre-processed to eliminate this inclination effect in our newly suggested method and, therefore, the result of RI calculation was more accurate in the fully automatic method as opposed to the semi-automatic method.

In Fig. 4, we present the results of time measurements required for initialization and index calculation (including initialization) using semi-automatic and fully automatic methods. The average time required for initialization was 28.12 s with the semi-automatic method and 0.07 s with the fully automatic method, while the average time required for index calculation was 61.12 s using the semi-automatic method and 30.09 s using the fully automatic method. Processing time enhancement was 99.75% at initialization process and 50.76% at whole index calculation process using the proposed fully automatic algorithm.

4 Discussion

ACM has been used as a characteristic tool for image segmentation and object tracking for past 20 years [7, 10, 16, 17]. Most studies focused on the improvement of segmentation and tracking performances of ACM to make it a more efficient diagnostic instrument, however, ACM initialization was relatively less spotlighted issues. Although several groups have carried out investigations regarding auto-initialization of ACM [10, 11, 14, 15], its clinical application to diagnose pre- and postoperative evaluation of surgery was rarely reported. Furthermore, fully automated index calculation methods for diagnosis of chest-wall deformity of funnel chest patient have not been previously reported. In applying the auto-initialization algorithm proposed in this article, we were able to demonstrate that (1) whole index calculation processes were fully automated, which enhanced calculation reliability and reproducibility; (2) whole processing time is drastically improved compared with previous manual and semi-automatic methods, and (3) training process is simplified, which improved clinical utility and feasibility of the algorithm.

Results of ACM initialization effect accuracy and reliability of the index calculation; that is, the calculated index value can differ according to the various settings of initialization processes. Thus, it is important to establish a unified initialization protocol and to minimize possibilities of variation from manual procedures to calculate targeted

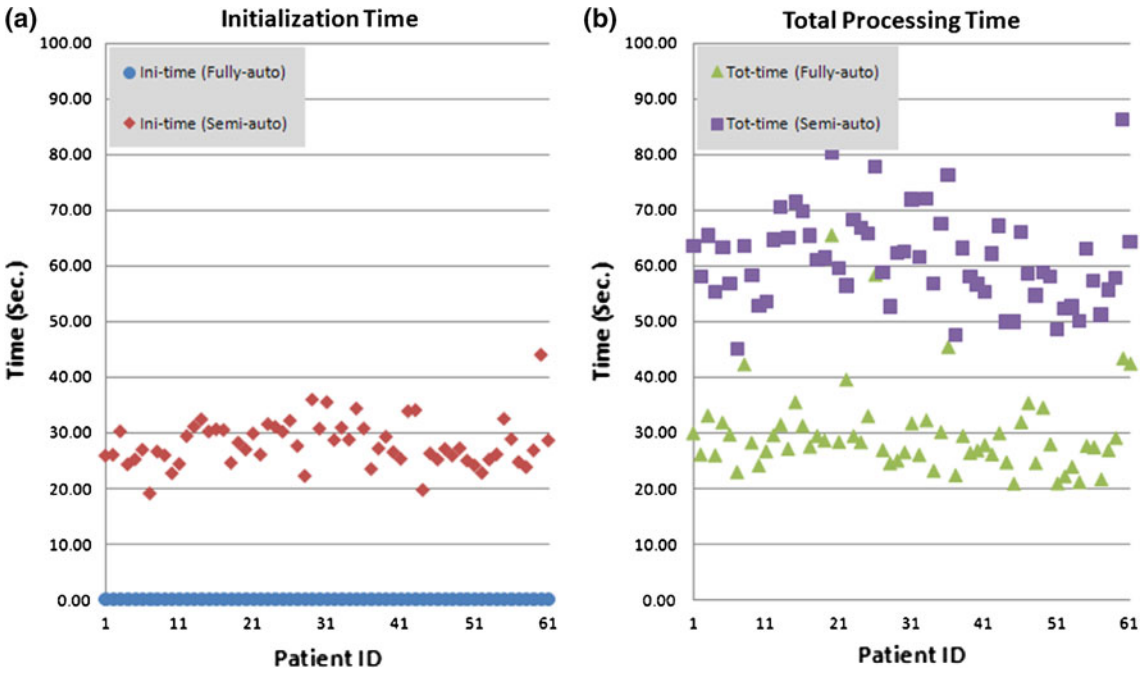

Fig. 4 Comparison results of processing time by the fully automatic method and the semi-automatic method in CT images of funnel chest patients. **a** Time required for initialization and **b** total required time

index with increased accuracy and reliability. The proposed algorithm eliminates manual intervention from whole index extraction processes and consequently, identical results can be obtained from the same input image every time; that is, this fully automated algorithm can be a highly reliable decision supporting tool for diagnosing funnel chest patients.

In order to segment whole chest-wall boundary using the fully automated algorithm, an initial boundary curve must be created from the result of the registration process which separates the lung, rib, sternum, and vertebra. In order to acquire accurate boundary information of each organ, noise elements in the CT image must be eliminated before registration. In most cases, noise elements were eliminated successfully by applying a Gaussian filter to the histogram of the CT image, however, when the original CT image is not clear intrinsically, HU values must be adjusted carefully to extract accurate boundary information. In this study, we present proper values of HU manually according to the clearance of each image, but an intelligent HU setting algorithm that determines the appropriate HU value automatically will be investigated in more detail in future studies.

Our currently developed algorithm first extracts bone (from rib, sternum, and vertebra) and lung area information by histogram analysis and then, additionally extracts their boundary information using a boundary search process. In order to reduce the time consumed for the boundary search process, we reduced the size of the image before auto-initialization by adopting the concept of multi-resolution. In some CT images, abnormal conversion of initial values from low-resolution image to high-resolution images was detected. In order to solve this problem, we need to improve the present multi-resolution method or apply new image conversion techniques.

In order to minimize the entire time required for index calculation, the time required for GVF field creation and ACM deformation must also be reduced. Time for ACM deformation can be reduced by auto-initialization, however, to reduce the time for GVF field creation, improvement of ACM itself is indispensable. In future studies, improvement of the fully automated ACM algorithm or development of new image segmentation techniques will be examined to reduce whole processing time for index calculation.

In previous study [8], we verified statistical correlation between new indices and HI, however, accuracy of new indices themselves were not verified. In further study, we have a plan to compare accuracy and reproducibility of new indices and HI quantitatively, and to extract threshold values of each index that can be used as a diagnostic guideline in clinical field. Further, we have additional plan to devise more accurate and reliable indices that can measure chest-wall deformity automatically.

5 Conclusion

In this study, we suggested a fully automatic algorithm that can measure the degree of chest-wall deformity by automating the initialization processes and verified its performance using CT images from funnel chest patients for evaluation. The experimental results demonstrated clinical feasibility of the proposed algorithm, such as enhanced precision, reduced processing time, and ease of use. Applying the proposed algorithm is expected to facilitate more efficient diagnosis and evaluation processes of funnel chest patients for clinical doctors.

Acknowledgments This research was supported by the Korea Electrotechnology Research Institute (KERI) grant funded by the Korean Government (No. 09-01-N0901-04).

References

1. Chang PY, Hsu ZY, Lai JY, Wang CJ, Ching YT (2010) Increase in intrathoracic volume in pectus excavatum patients after the Nuss procedure. Med Biol Eng Comput 48:133–137
2. de Matos AC, Bernardo JE, Fernandes LE, Antunes MJ (1997) Surgery of chest wall deformities. Eur J Cardiothorac Surg 12:345–350
3. Donnelly LF, Frush DP (1999) Abnormalities of the chest wall in pediatric patients. AJR Am J Roentgenol 173:1595–1601
4. Golladay ES, Golladay GJ (1997) Chest wall deformities. Indian J Pediatr 64:339–350
5. Haller JA Jr, Kramer SS, Lietman SA (1987) Use of CT scans in selection of patients for pectus excavatum surgery: a preliminary report. J Pediatr Surg 22:904–906
6. Haller JA Jr, Scherer LR, Turner CS, Colombani PM (1989) Evolving management of pectus excavatum based on a single institutional experience of 664 patients. Ann Surg 209:578–582 discussion 82-3
7. Kass M, Witkin A, Terzopoulos D (1988) Snakes: active contour models. Int J Comput Vis 1:321–331
8. Kim HC, Park HJ, Ham SY, Nam KW, Choi SY, Oh JS et al (2008) Development of automatized new indices for radiological assessment of chest-wall deformity and its quantitative evaluation. Med Biol Eng Comput 46:815–823
9. Lee CS, Park HJ, Lee SY (2004) New computerized tomogram (CT) indices for pectus excavatum: tools for assessing modified techniques for asymmetry in Nuss repair. Chest Suppl 126(4):777s
10. Li B, Acton S (2008) Automatic active model initialization via Poisson inverse gradient. IEEE Trans Image Process 17:1406–1420
11. Li C, Liu J, Fox M (2005) Segmentation of external force field for automatic initialization and splitting of snakes. Pattern Recognit 38:1947–1960
12. Ohno K, Nakahira M, Takeuchi S, Shiokawa C, Moriuchi T, Harumoto K et al (2001) Indications for surgical treatment of funnel chest by chest radiograph. Pediatr Surg Int 17:591–595
13. Ohno K, Morotomi Y, Nakahira M, Takeuchi S, Shiokawa C, Moriuchi T et al (2003) Indications for surgical repair of funnel chest based on indices of chest wall deformity and psychological state. Surg Today 33:662–665
14. Tauber C, Batatia H, Ayache A, CNRS Institute Toulouse France (2005) A general quasi-automatic initialization for snakes:

application to ultrasound images. In: IEEE international conference on image processing, pp 806–809
15. Xingfei G, Jie T (2002) An automatic active contour model for multiple objects. In: 16th International Conference on Pattern Recognition (ICPR'02), pp 881–884
16. Xu C, Prince JL (1998) Snakes, shapes, and gradient vector flow. IEEE Trans Image Process 7:359–369
17. Xu C, Prince JL (1998) Generalized gradient vector flow external forces for active contours. Signal Process 71:131–139